Check for updates

New Phytologist

Research

Dynamic soil hydraulic resistance regulates stomata

Anju Manandhar[1], Ian M. Rimer[1], Talitha Soares Pereira[1], Javier Pichaco[2], Fulton E. Rockwell[3] and Scott A. M. McAdam[1]

[1]Department of Botany and Plant Pathology, Purdue University, West Lafayette, IN 47907, USA; [2]Irrigation and Crop Ecophysiology Group, Instituto de Recursos Naturales y Agrobiología de Sevilla (IRNAS, CSIC), Ave Reina Mercedes 10, 41012, Seville, Spain; [3]Department of Organismic and Evolutionary Biology, Harvard University, Cambridge, MA 02138, USA

Author for correspondence:
Scott A. M. McAdam
Email: smcadam@purdue.edu

Received: *6 June 2024*
Accepted: *5 July 2024*

New Phytologist (2024)
doi: 10.1111/nph.20020

Key words: drought, embolism, plant hydraulics, rhizosphere, roots, stomata, transpiration.

Summary

- The onset of stomatal closure reduces transpiration during drought. In seed plants, drought causes declines in plant water status which increases leaf endogenous abscisic acid (ABA) levels required for stomatal closure. There are multiple possible points of increased belowground resistance in the soil–plant atmospheric continuum that could decrease leaf water potential enough to trigger ABA production and the subsequent decreases in transpiration.
- We investigate the dynamic patterns of leaf ABA levels, plant hydraulic conductance and the point of failure in the soil–plant conductance in the highly embolism-resistant species *Callitris tuberculata* using continuous dendrometer measurements of leaf water potential during drought.
- We show that decreases in transpiration and ABA biosynthesis begin before any permanent decreases in predawn water potential, collapse in soil–plant hydraulic pathway and xylem embolism spread.
- We find that a dynamic but recoverable increases in hydraulic resistance in the soil in close proximity to the roots is the most likely driver of declines in midday leaf water potential needed for ABA biosynthesis and the onset of decreases in transpiration.

Introduction

Transpired water loss from plants is an inevitable consequence of gas exchange for carbon capture and photosynthesis (Curtis, 1926; Penman, 1952). The opening and closing of stomatal pores on leaf surfaces regulate this gaseous exchange between the plant and the atmosphere, with stomatal closure being the primary mechanism for reducing transpiration, limiting excessive water loss and avoiding hydraulic failure when drought depletes soil water reserves. The trigger and timing of when stomata begin to close is essential for the accurate modelling of plant and ecosystem responses to climate, as well as terrestrial carbon, water and energy fluxes. Considerable work over the past century has found that the level of dehydration at which stomatal closure occurs is a highly adaptive trait, varying considerably across species and ecosystems (Brodribb & Holbrook, 2003; Martínez-Vilalta & Garcia-Forner, 2017; Rockwell & Holbrook, 2017). While quite variable across species, woody plants adapted to the driest environments tend to close stomata at lower water potentials than herbaceous species native to mesic environments (Jin *et al.*, 2023). Fern and lycophyte species, many of which are confined to wet and humid environments, have stomata that are highly sensitive to declines in leaf water status compared with seed plants (Brodribb & Holbrook, 2004). Given the importance of stomatal closure during drought, determining the trigger of this response is a critical endeavor (Anderegg *et al.*, 2013; Verslues *et al.*, 2023).

Declining transpiration, caused by reduced stomatal conductance, occurs during drought because of decreased plant water status. In seed plants, a decline in mesophyll cell turgor pressure triggers abscisic acid (ABA) biosynthesis, closing stomata during drought (Pierce & Raschke, 1980; McAdam & Brodribb, 2016). The decline in plant water status is an inevitable consequence of declining soil water status, but the cause is much debated. Somewhere along the soil–plant–atmosphere continuum (SPAC) an increased resistance to water flow leads to a decrease in downstream water potentials. Potential key resistors to water flow during drought include pathways through the soil itself, the soil-to-root interface, the exodermis, cortex or endodermis of the roots, the xylem, the bundle sheath, or mesophyll of the leaf and the stomata. There are a range of hypotheses, and experimental evidence that propose each one of these resistors could be the dominant driver of leaf water status decline and the onset of stomatal closure during drought.

Among the possible aboveground resistors triggering stomatal closure, increased resistance in the xylem caused by embolism is the least likely since the formation of embolism leads to the rapid, and often unrecoverable, desiccation of downstream tissue (Hochberg *et al.*, 2017; Creek *et al.*, 2020). The other hypothesized aboveground resistors in the hydraulic pathway upstream of stomata during drought remain debated. Decreased conductance outside the xylem (K_{ox}) of the leaf over mild changes in water potential has been observed in some angiosperm species and linked to stomatal closure at high vapor pressure deficit (VPD)

© 2024 The Author(s).
New Phytologist © 2024 New Phytologist Foundation.
This is an open access article under the terms of the Creative Commons Attribution License, which permits use, distribution and reproduction in any medium, provided the original work is properly cited.

(Shatil-Cohen *et al.*, 2011; Torres-Ruiz *et al.*, 2015; Hernandez-Santana *et al.*, 2016; Scoffoni *et al.*, 2023). But rehydration kinetics of leaves suggests that declines in leaf hydraulic conductance (K_{leaf}) are likely to occur only when embolism begins to form during drought (Brodribb *et al.*, 2003; Smith-Martin *et al.*, 2020; although cf. Trifiló *et al.*, 2016; Scoffoni *et al.*, 2017). Recent work also suggests that there is no decline in within-plant hydraulic conductance when VPD increases (Brodribb & Cochard, 2009; Martins *et al.*, 2016; Bourbia & Brodribb, 2024) and that K_{ox} is driven by xylem water potential (Jain *et al.*, 2023). Declines in K_{ox} have not been linked to when stomata start closing during drought, and the phenomenon may have even evolved to keep stomata open in the early stages of drought (Jain *et al.*, 2023).

The importance of belowground resistors to water flow in the SPAC that drive declines in leaf water potential (Ψ_{leaf}) and trigger stomata to start closing during drought is also highly debated. Belowground hydraulic resistance (the inverse of conductance) is a function of the resistance through the root, and the interface between the roots and the soil, and the soil itself (Steudle & Peterson, 1998). The estimates of the vulnerability of roots to embolism have a wide range, with evidence of variable failure beginning at relatively hydrated water potentials in the monocot *Triticum aestivum* (Harrison Day *et al.*, 2023), while other studies suggest roots are highly embolism resistant in woody angiosperms (Rodriguez-Dominguez *et al.*, 2018; Skelton *et al.*, 2019). The cell-to-cell resistance to water flow might arise from the necessity for active, symplastic root water uptake, where flow depends on aquaporins, especially due to cell layers that are suberized or lignified (Vandeleur *et al.*, 2009), yet this remains difficult to experimentally distinguish from passive symplastic pathways (Steudle & Peterson, 1998; Li *et al.*, 2014). There have also been many studies that point to a decline in conductance outside the xylem in the roots (K_{rox}) because of root shrinkage (Passioura, 1988), and even lacunae formation in the cortical region (North & Nobel, 1991; Cuneo *et al.*, 2016). A reversible collapse of cortical cells and an increase in root–soil disconnect have also been attributed to declines in root-to-soil interface conductance (K_i) (Bourbia *et al.*, 2021). In the roots of woody plants, an additional decrease in K_i might also occurs because of drought-induced suberization decreasing root permeability to water (Zimmermann *et al.*, 2000). These belowground decreases in K_{rox} and K_i have all been linked to stomatal closure (Rodriguez-Dominguez & Brodribb, 2020; Bourbia *et al.*, 2021; Yang *et al.*, 2023). In addition to declines in K_{rox} and K_i, regulation of stomatal conductance (g_s) has also been linked to declines in soil hydraulic conductance, in the soil in closest proximity to the roots (K_z) and the bulk soil (K_s) (Carminati & Javaux, 2020; Koehler *et al.*, 2022). Stomatal closure appears to occur at a threshold bulk soil water potential which in turn feeds-back on reducing rapid decreases in K_z and K_s (Carminati & Javaux, 2020; Koehler *et al.*, 2022). Belowground declines in hydraulic conductance remain experimentally unlinked to leaf ABA biosynthesis and whole plant transpiration decline during a drought.

Most of our understanding of stomatal closure during drought is documented through the lens of plant water status. Drought-induced stomatal closure occurs exponentially with decreasing Ψ_{leaf} (Jarvis, 1976; Dewar, 2002; Tardieu *et al.*, 2015; Martínez-Vilalta & Garcia-Forner, 2017). Though gradual stomatal closure during drought is apparent in the relationship between g_s and Ψ_{leaf}, the Ψ_{leaf} at which stomata begin regulating transpiration cannot be clearly resolved from these analyses. The onset of stomatal regulation early in a drought can delay large decreases in whole plant water status (Buckley, 2019; Wankmüller & Carminati, 2022; Manandhar *et al.*, 2023). Thus an exponential relationship between g_s and Ψ_{leaf} over a hydrated range of Ψ_{leaf} is often observed. ABA-mediated stomatal regulation often begins before large declines in both predawn and midday Ψ_{leaf} (Manandhar *et al.*, 2023). Given that stomatal closure during drought is a gradual decrease in daily maximums; where resistance somewhere in the SPAC sets this daily decline in maximum g_s, we hypothesize that there is a diurnally-\recoverable decline in conductance that allows gradual ABA-mediated stomatal closure. This stomatal closure occurs before, and delays, subsequent precipitous and unrecoverable declines in conductance in the SPAC at low Ψ_{leaf}.

We used *Callitris tuberculata* R.Br. ex R.T.Baker et H.G.Smith (Cupressaceae) to test this hypothesis, because it is reported to have the most embolism-resistant xylem of any species measured to date (Larter *et al.*, 2017), and species from this genus display no declines in K_{leaf} during VPD transitions (Bourbia & Brodribb, 2024), or when Ψ_{leaf} declines before embolism formation (Brodribb & Cochard, 2009), suggesting that K_{ox} remains constant during dehydration. The highly resistant, aboveground conductance to dehydration makes this species an ideal model system in which to investigate the role of belowground resistances in regulating stomatal responses during drought. We used gravimetric soil water content (gSWC) as a scale for bulk soil drought and continuously monitored Ψ_{leaf} using optical dendrometers (Bourbia *et al.*, 2021) during drought; we also developed a method to measure the resistance to water flow between the plant and the soil. By this approach, we were able to determine which of the key resistances in the SPAC primarily drive declines in Ψ_{leaf}, triggering ABA biosynthesis, and thus the onset of stomatal closure during drought. We present a new understanding of the sequence of key events in the SPAC as drought progresses.

Materials and Methods

Five-year-old *Callitris tuberculata* (Cupressaceae) plants were grown from seed in 5-l pots in a glasshouse under natural light. The growth conditions were set to a day : night temperature of 22°C : 19°C. Pots contained a 1 : 1 mix of sand and Indiana Miami topsoil (a fine-loamy, mixed, active, mesic Oxyaquic Hapludalf). The final mix consisted of a particle size distribution of 87% sand, 5% silt and 8% clay. Plants were watered daily and fertilized weekly with a liquid fertilizer solution (Miracle-Gro Water-soluble All Purpose Plant Food; Scotts Co., LLC, Marysville, OH, USA). Experiments were conducted in November 2022 on plants with a well-established root system that fully

© 2024 The Author(s).
New Phytologist © 2024 New Phytologist Foundation.

14698137, 0, Downloaded from https://nph.onlinelibrary.wiley.com/doi/10.1111/nph.20020 by Readcube (Labtiva Inc.), Wiley Online Library on [26/08/2024]. See the Terms and Conditions (https://onlinelibrary.wiley.com/terms-and-conditions) on Wiley Online Library for rules of use; OA articles are governed by the applicable Creative Commons License

14698137, 0, Downloaded from https://nph.onlinelibrary.wiley.com/doi/10.1111/nph.20020 by Readcube (Labtiva Inc.), Wiley Online Library on [26/08/2024]. See the Terms and Conditions (https://onlinelibrary.wiley.com/terms-and-conditions) on Wiley Online Library for rules of use; OA articles are governed by the applicable Creative Commons License

explored the soil volume ($21.4 \pm 2.18\ g\ l^{-1}$ root dry weight per volume) to ensure minimal heterogeneity in soil water distribution as the soil dried.

Drought treatment

A progressive drought was imposed on five plants, while three additional plants were maintained as well-watered controls. The night before the drought experiment was implemented, all pots were watered to saturation and allowed to drain overnight. The next morning, after excess water had stopped draining, pots were double bagged and sealed around the base of the stem with a releasable zip-tie to prevent water loss from the soil. Plants were then weighed to define total pot weight at 100% pot capacity (PW_{pc}). Water loss from transpiration was measured as the difference in pot weights taken daily at the same time in the afternoon. For the well-watered control treatment, plants were watered daily so that pot weight was returned to a weight within 200 g of pot capacity (*c.* 90% of total available water at pot capacity). For the first 2–3 d after bagging, all plants were re-watered daily and maintained at well-watered conditions. The progressive drought was imposed by withholding water. Before decreases in g_s occurred (when transpiration was maximum) in the early stages of drought, water was added only when 24 h transpiration was maximum, ensuring no $>$ 200 g pot weight was lost per day, in an attempt to mimic the onset of a gradual, natural drought event. This approach allowed gradual declines in gSWC before stomata started to close.

At the end of the drought experiment, the last recorded pot weight was considered the final pot weight (PW_f). Subsamples of *c.* 30 g of soil were destructively collected, weighed and oven dried at 105°C for at least 3 d and reweighed. The ratio of the water content in fresh soil to the weight of dry soil was used to determine gSWC at PW_f ($gSWC_f$). Plants were then watered to PW_{pc}, another subsample of soil was taken, weighed, oven dried and reweighed to determine gSWC at pot capacity ($gSWC_{pc}$). The pot available soil water (PAW) for each day during the experiment was considered the difference between pot weight and PW_f. The gSWC for each day was found using the day's PAW and the ratio of the difference between the two measured gSWC ($gSWC_{pc} - gSWC_f$) to the difference between the corresponding PAW values at PW_{pc} and PW_f.

Total transpiration for every 24 h period (T_{dt}) was found from the daily decrease in pot weight corrected for the weight of any water added. Midday transpiration (T_{md}) was measured as the difference between pot weights over 2 h spanning solar noon. To account for day-to-day variation in transpiration due to differences in environmental conditions (particularly maximum light intensity), the transpiration ratio (TR) was calculated as:

$$TR = \frac{T_{dt}}{\text{Mean transpiration of well watered plants}}$$

To visualize the effects of drought on transpiration beyond the variation caused by differences between individuals, relative transpiration was calculated as:

$$\text{Relative transpiration} = \frac{TR}{\text{Mean pot TR of the first 3 d}}$$

Midday canopy conductance was calculated from T_{md}, leaf area (measured at the end of each experiment) and average VPD obtained from humidity and air temperature data collected at canopy height logged every minute (Dragino LHT65 Temperature & Humidity sensor; Dragino Technology Co. Ltd, Shenzhen, China), leaf temperature was assumed to match air temperature because the air in the room was well circulated using overhead fans. To find the leaf area of each plant, the leaf mass per unit area (LMA) was first found for 20 branches from five plants (five branches per plant). At the end of each experiment, the full canopy of leaves was harvested and oven dried at 70°C for at least 72 h, after which the leaf dry mass was measured. The canopy leaf area was calculated from the canopy dry mass and LMA.

Quantification of ABA levels during drought

Every second day a small branch was harvested from each plant for ABA quantification and Ψ_{leaf} measurement. Ψ_{leaf} was measured using a Scholander pressure chamber, after slow depressurization, tissue was taken for ABA quantification. Around 100 mg was weighed and immediately transferred to a 50-ml falcon tube and covered with 5–7 ml of cold (−20°C) 80% aqueous methanol (v/v) with added $250\ mg\ l^{-1}$ butylated hydroxytoluene. The branch was roughly chopped and stored at −20°C. Samples were then homogenized thoroughly, and 15 ng of labeled [$^2H_6$]-ABA was added to each sample as an internal standard. ABA was extracted overnight at 4°C, following which an aliquot of the supernatant was dehydrated at 40°C. Once dried, the leaf extraction was resuspended in 200 µl of 2% acetic acid in water (v/v) and centrifuged, and the ABA levels were measured using liquid chromatography tandem mass spectrometry (Agilent 6460, QQQ LC-MS; Aglient Technologies, Inc., Santa Clara, CA, USA).

Monitoring leaf water potential with optical dendrometers

For continuous Ψ_{leaf} measurements, leaf dendrometers (one per plant) were installed in the upper canopy to image specific segments of the cylindrical branches that terminated in a male cone, every 5 min for the duration of the drought in all plants (Bourbia *et al.*, 2021). The relationship between stem widths and the Ψ_{leaf} measured using the Scholander chamber was then used to find the dendrometer-derived Ψ_{leaf} during the drought treatment (Supporting Information Fig. S1).

Pressure–volume curves

Pressure–volume (PV) curves were made from the relationship between branch relative water content and Ψ_{leaf}, for three branches following the method of Tyree & Hammel (1972). A relationship between leaf turgor potential (Ψ_p) and Ψ_{leaf} was made (Fig. S2) using the PV relationships to calculate the average Ψ_p for each dendrometer-derived Ψ_{leaf}.

© 2024 The Author(s).
New Phytologist © 2024 New Phytologist Foundation.

Nighttime rehydration to determine soil and plant conductance

The dynamics of nighttime Ψ_{leaf} recovery was observed in plants maintained at or above pot capacity and through progressive drought. As gSWC declined, plants were observed to have two phases of Ψ_{leaf} recovery: the first phase occurred immediately after stomatal closure at night and was a rapid relaxation of Ψ_{leaf}; this was followed by the second phase which occurred with an abrupt decrease in slope and was never observed in plants sustained above PW_{pc}. We considered this second phase to reflect a slowly recharging gradient in water potential between the soil and the leaf. The Ψ_{leaf} dynamics during this second phase, until maximum Ψ_{leaf} was observed before stomatal opening at dawn, was used to determine the conductance through the soil and the plant ($K_{effective}$). Since $K_{effective}$ includes the conductance from the water source in the soil to the leaf, it includes K_s, K_i and the conductance through the plant, K_{plant}:

$$\frac{1}{K_{effective}} = \frac{1}{K_{plant}} + \frac{1}{K_i} + \frac{1}{K_s}$$

$K_{effective}$ was calculated based on the principle that water flows through a series of resistors to recharge a capacitor (the leaf) (Brodribb & Holbrook, 2004) as:

$$K_{effective} = -\log_e\left(\frac{\Psi_t - \Psi_{pd}}{\Psi_{gs0} - \Psi_{pd}}\right)\frac{C}{t}$$

where C is the average leaf capacitance measured from the branch PV curves. Ψ_{leaf} at nighttime stomatal closure (Ψ_{gs0}) found from the inflection point of the two phases of Ψ_{leaf} recovery. t is the time between Ψ_{gs0} and when $K_{effective}$ was calculated. Ψ_t is the Ψ_{leaf} corresponding to time, t. Ψ_{pd} is the Ψ_{leaf} at predawn or the highest water potential reached at night. $K_{effective}$ was measured for two time points every night during the drought, at postdusk, an hour after the inflection point where the second phase of leaf rehydration began and at predawn, 30 min before dawn. $K_{effective}$ was also measured for plants in saturated soils only for the postdusk period since the second slow phase of Ψ_{leaf} recovery was absent and Ψ_{pd} was achieved within 6 h past dusk (Fig. S3). To determine Ψ_{gs0} for plants in saturated soils, the time when transpiration reached a minimum was determined from continuous balance measurements and postdusk $K_{effective}$ an hour after Ψ_{gs0} was found.

Resistance to water flow from plant to soil

To measure the resistance to water flow between roots and soil during drought, 14 additional plants were exposed to a drought treatment and the resistance to water flow between roots and soil were measured at a Ψ_{pd} ranging from −0.57 to −8.06 MPa. To determine the resistance to water flow from roots to soil, we measured the flow of water from an instantaneously rehydrated plant into the soil. For each plant slated for measurements, Ψ_{pd} was measured as a proxy for the bulk soil water potential. The pot was weighed, and the canopy was removed at the base of the main stem. The excised stem, protruding from the bagged pot, was immediately recut under water to remove embolized tracheids. While still submerged, a Tygon plastic hose filled with water was securely attached to the cut end of the stem. The other end of the hose, filled with water, was suspended in a conical flask placed on a scale (EK-410i; A&D Co. Ltd, Ann Arbor, MI, USA) continuously logging data onto an attached desktop. Retort stands and clamps were used to support the tube to ensure that the weight of the tubing did not influence the reading on the balance. The plant and balance were then covered with a box to reduce airflow disturbance.

The balance reading of water uptake from the flask into the stem, root and soil system was recorded continuously every minute. Water uptake was measured for at least 1000 min, and this time was not sufficient for soil to reach saturation based on pot weight values. The uptake rate ($\mu mol\ s^{-1}\ g^{-1}$ (DW of roots)) from the root system to the soil was calculated for the last 240 min, to ensure flow rates were stable, and normalized by root dry weight (to be described later). The resistance to water flow from the root to the soil was determined as:

$$\text{Root to soil hydraulic resistance} = \frac{\Psi_{pd}}{\text{Uptake rate}}$$

After uptake measurements were made, the pot was disconnected from the water supply. The soil was allowed to equilibrate overnight, the pot was weighed, and a subsample of soil was collected for $gSWC_f$ measurement. The soil was watered and returned to PW_{pc} overnight. In the morning, another subsample of soil was collected to measure $gSWC_{pc}$. The gSWC of the soil before the root-to-soil rehydration was calculated as described above. The soil was then gently washed from the roots, and the roots were dried in an oven for at least 72 h at 70°C to measure dry weight.

To ensure that the observed uptake of water was drawn into the soil and was not just recharging a potential large root capacitor, another control experiment was conducted with five plants. These plants were subjected to a drought treatment. Ψ_{pd} was measured for plants at varying levels of soil water status. While the plants were still equilibrated in dark conditions, the pots were first weighed, and then, soil was gently dusted and removed from the roots. A subsample of soil was collected for $gSWC_f$ determination. The exposed, soil-free roots were placed in a large bag, which was sealed around the stem at the base of the plant. The plant was then cut at the base of the stem. The stem, still attached to the roots without soil, was recut underwater following the same steps described above to measure water flow into the roots. The uptake of water from the flask into the roots was measured over the same period as in plants with soil intact. At the end, a subsample of root was taken to determine water potential and ensure full rehydration of tissue (all samples had a water potential close to 0 MPa), and the roots were washed and dried in the oven to determine root dry weight. For these five plants, since the pots could not be re-watered to pot capacity for $gSWC_{pc}$, the average $gSWC_{pc}$ for the rest of the plants at pot capacity was used.

© 2024 The Author(s).
New Phytologist © 2024 New Phytologist Foundation.

14698137, 0, Downloaded from https://nph.onlinelibrary.wiley.com/doi/10.1111/nph.20020 by Readcube (Labtiva Inc.), Wiley Online Library on [26/08/2024]. See the Terms and Conditions (https://onlinelibrary.wiley.com/terms-and-conditions) on Wiley Online Library for rules of use; OA articles are governed by the applicable Creative Commons License

14698137, 0, Downloaded from https://nph.onlinelibrary.wiley.com/doi/10.1111/nph.20020 by Readcube (Labtiva Inc.), Wiley Online Library on [26/08/2024]. See the Terms and Conditions (https://onlinelibrary.wiley.com/terms-and-conditions) on Wiley Online Library for rules of use; OA articles are governed by the applicable Creative Commons License

Optical vulnerability to embolism

Embolism formation in the xylem of the stem was determined in four representative individuals using the optical method as described by Brodribb *et al.* (2017). The relationship between percent embolized xylem area in the main stem and Ψ_{leaf}, which was measured periodically (every 6 h) in adjacent stems and continuously with a psychrometer attached to the main stem (ICT International, Armidale, NSW, Australia), was constructed for each individual.

Modelling soil hydraulic vulnerability

The hydraulic vulnerability of the soil used in the experiment was determined according to the Maulem-Van Genuchten model using HYDRUS-1D (PC-Progress, Prague, Czech Republic). The soil texture parameters of 87% sand, 5% silt and 8% clay, without specifying bulk density, were used in the Rosetta pedotransfer function.

Testing for aquaporin control of nighttime Ψ_{leaf} relaxation

In two individuals of *C. tuberculata*, soil was gently removed from roots and placed into a bucket containing 10 l of water and an aerator. A dendrometer was fixed to a male cone-bearing shoot in the upper canopy, and Ψ_{leaf} was measured continuously. After a day of acclimation in the hydroponic system, before dusk, silver nitrate was added to the water (final concentration 200 μM) to inhibit root aquaporins. Ψ_{leaf} was tracked for the next 48 h.

Results

Transpiration declines as foliar ABA levels increase

During drought, we first observed declines in transpiration and canopy conductance. Relative transpiration remained stable until gSWC reached 0.14 g g^{-1} (95% CI: 0.15–0.13 g g^{-1}) (Fig. 1a) at which it declined, with the relationship between relative transpiration and gSWC found to fit a two-segmented linear relationship. At 0.06 g g^{-1} gSWC, relative transpiration had decreased to 10% of maximum.

Measurements of Ψ_{leaf} from the Scholander pressure chamber had a strong linear relationship with relative branch dendrometer widths (Fig. S1) with an R^2 of 0.98 and the *P*-value of the coefficient was < 0.001. Relative transpiration, as a function of dendrometer-midday Ψ_{leaf} (Ψ_{md}), declined exponentially (Fig. 1b; Relative transpiration $= 1.6e^{0.53\Psi_{md}}$, $R^2 = 91$). Similarly, we found midday canopy conductance declined exponentially with dendrometer Ψ_{md} (Fig. 1b inset, canopy conductance $= 197e^{0.5\Psi_{md}}$, $R^2 = 0.85$). Midday, maximum canopy conductance fluctuated between 59 and 163 mmol m^{-2} s^{-1} when gSWC was higher than 0.14 g g^{-1}, after which it declined (Fig. S4).

Foliar ABA levels at hydrated gSWC levels were low at an average of 7.06 μg g^{-1} DW ± 1.17 (SE), until declines in transpiration began at *c.* 0.14 g g^{-1} gSWC, after which leaf ABA levels increased (Fig. 1a). The increase in leaf ABA level with decreasing gSWC was visualized with a locally linear smoothing regression. During the driest period where gSWC levels were lower than 0.05 g g^{-1}, ABA levels increased to an average of 14.33 μg g^{-1} DW ± 0.62. Relative transpiration correlated with foliar ABA levels during drought, declining according to a sigmoidal relationship as foliar ABA levels increased (Fig. S5).

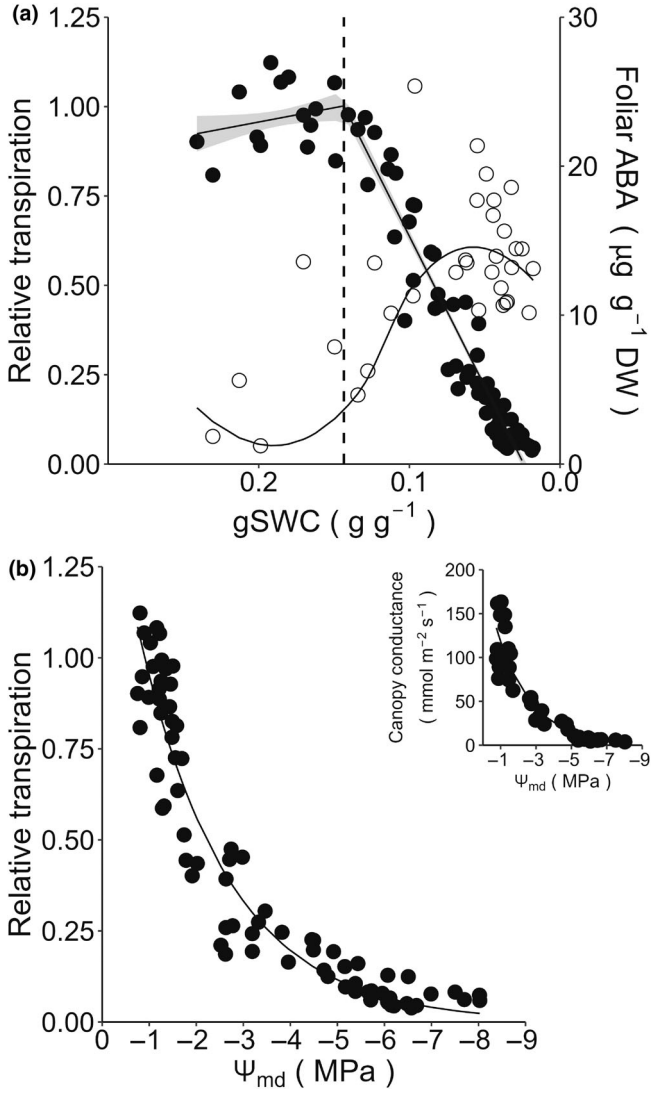


Fig. 1 The onset of stomatal closure coincides with an increase in leaf abscisic acid (ABA) levels. (a) Daily transpiration relative to plants under well-watered conditions (black) and ABA levels (white) as gravimetric soil water content (gSWC) declines in *Callitris tuberculata* ($n = 5$ individuals). The relationship between relative transpiration and gSWC is summarized as a two-segmented linear regression (SEGMENTED package, v.2.0-0; Muggeo, 2008), with the dashed line representing the gSWC breakpoint (0.14 g g^{-1}) between the segments; the shaded region depicts the SE of the predicted relative transpiration. The trend of ABA increase is represented by a loess (locally linear smoothing) regression with the SE as the shaded region. (b) The relationship between relative transpiration and dendrometer-midday leaf water potential Ψ_{md} ($n = 5$ individuals). The insert depicts the relationship between midday canopy conductance and Ψ_{md}. The relationships between relative transpiration or canopy conductance and Ψ_{md} are represented by exponential regressions.

© 2024 The Author(s).
New Phytologist © 2024 New Phytologist Foundation.

Increasing predawn-midday water potential differential closes stomata

The relationship between gSWC and both dendrometer Ψ_{pd} and Ψ_{md}, fit two-segmented linear regressions (Fig. 2a). Ψ_{pd} remained high and only declined by 0.07 MPa with every 0.1 g g^{-1} decrease in gSWC until gSWC declined past 0.086 g g^{-1} (95% CI: 0.094–0.079), after which Ψ_{pd} declined by 8.4 MPa with every 0.1 g g^{-1} decrease in gSWC. Ψ_{md} also had a gradual decrease earlier in the drought with a 0.57 MPa decrease for every 0.1 g g^{-1} gSWC until the breakpoint of 0.083 g g^{-1} (95% CI: 0.089–0.077) gSWC, after which Ψ_{md} had an 8.6 MPa decline for every 0.1 g g^{-1} gSWC.

Due to the near absent decrease of Ψ_{pd} in the early stages of the drought, the gradient between Ψ_{pd} and Ψ_{md} ($\Delta\Psi_{pd\text{-}md}$) (Fig. 2b) increased linearly by 0.50 MPa for every 0.1 g g^{-1} decrease in gSWC, until the soil dried to 0.09 g g^{-1} (95% CI: 0.11–0.073) gSWC. After the threshold gSWC, the $\Delta\Psi_{pd\text{-}md}$ decreased by 0.86 MPa for every 0.1 g g^{-1} decline in gSWC. The increasing differential between Ψ_{pd} and Ψ_{md} early in drought resulted in a steady decrease in midday Ψ_p (Fig. 2c), while predawn Ψ_p remained constant. Predawn Ψ_p returned to well-watered levels for most of the drought until the steep decline around the gSWC where the $\Delta\Psi_{pd\text{-}md}$ also started to decrease.

The increasing $\Delta\Psi_{pd\text{-}md}$ during drought was also apparent in the continuous measurement of Ψ_{leaf} (Fig. 3a). Early in the drought, before gSWC crosses the threshold of transpiration decline between 0.16 and 0.13 g g^{-1}, minimum daily values of Ψ_{leaf} declined with each progressive day. During this time, Ψ_{leaf} relaxed to predawn levels overnight. Early nighttime relaxation of Ψ_{leaf} was rapid at dusk when stomata closed at night, after which the rate of Ψ_{leaf} increase shifted to a second phase and became more gradual until Ψ_{pd} were reached. This trend is only seen before gSWC reached 0.086 g g^{-1}, after which Ψ_{pd} started decreasing each progressive day of the drought. The two-phased Ψ_{leaf} relaxation at night was absent in plants maintained in saturated soils (Fig. S3).

Diurnally recoverable declines in soil-to-plant hydraulic conductance as transpiration declines

$K_{effective}$ after nighttime stomatal closure is high in saturated soils, and similar to the mean hydraulic conductance of the whole plant under well-watered conditions determined from transpiration and the differential between Ψ_{pd} and Ψ_{md}, which was 0.85 mmol m^{-2} s^{-1} MPa^{-1} (±0.27, $n = 4$). When the soil is not saturated, in all cases, the initial postdusk $K_{effective}$ is low and increases by predawn (Fig. 3b). This differential in $K_{effective}$ over the course of the night was present for the duration of the drought until the soil dried to 0.075 g g^{-1} gSWC. This gSWC corresponds to the point of the drought where Ψ_{pd} no longer recovered overnight (Fig. 2a). A model of K_s suggests that K_s declines rapidly at moderate soil water potentials (Fig. S6).

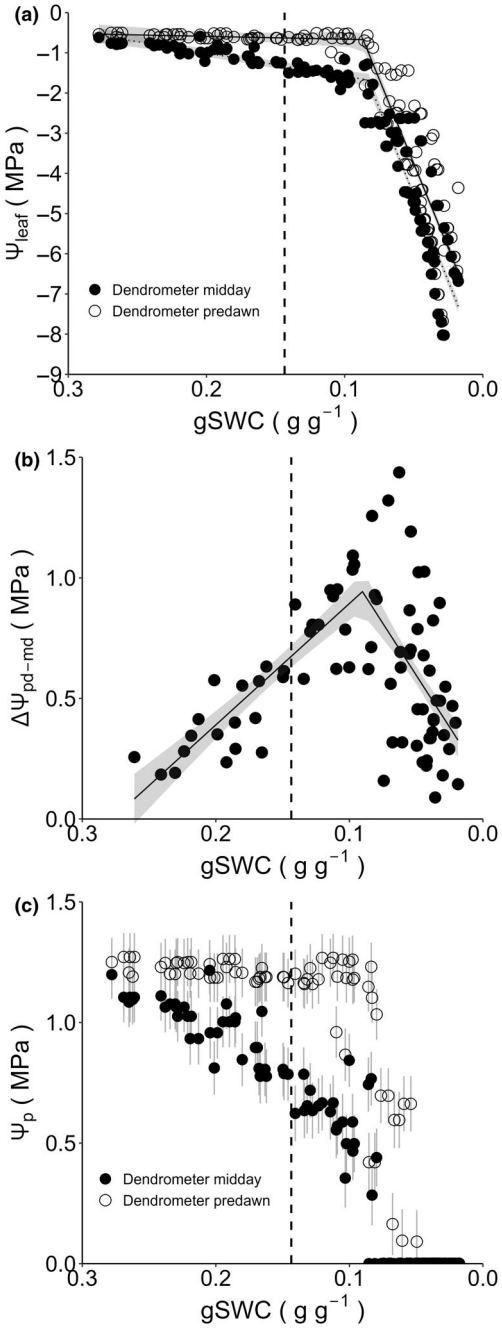


Fig. 2 An increasing differential between predawn and midday leaf water potentials (Ψ_{leaf}. MPa) drives declines in leaf turgor (Ψ_p) early in a drought. (a) Predawn (white) and midday (black) measured with the leaf dendrometer, as gravimetric soil water content (gSWC) declines during soil drought in *Callitris tuberculata* ($n = 5$ individuals). The mean decline in midday Ψ_{leaf} (solid black lines) and predawn Ψ_{leaf} (dotted lines), as gSWC declines are presented as two-segmented linear regressions with respective SE (shaded regions). (b) The differential between predawn and midday Ψ_{leaf}, $\Delta\Psi_{pd\text{-}md}$ (MPa) as gSWC declines during drought ($n = 5$ individuals). A two-segmented linear regression depicts the trends of $\Delta\Psi_{pd\text{-}md}$ as gSWC declines (solid line), with SE as the shaded region. (c) The mean leaf turgor potential (Ψ_p) with SE, calculated from pressure–volume relationships between Ψ_{leaf} and Ψ_p (Supporting Information Fig. S2), at midday (black) and predawn (white) as gSWC declines ($n = 5$ individuals). The dashed vertical line in all panels is the gSWC threshold at which relative transpiration begins to decline.

© 2024 The Author(s).
New Phytologist © 2024 New Phytologist Foundation.

14698137, 0, Downloaded from https://nph.onlinelibrary.wiley.com/doi/10.1111/nph.20020 by Readcube (Labtiva Inc.), Wiley Online Library on [26/08/2024]. See the Terms and Conditions (https://onlinelibrary.wiley.com/terms-and-conditions) on Wiley Online Library for rules of use; OA articles are governed by the applicable Creative Commons License

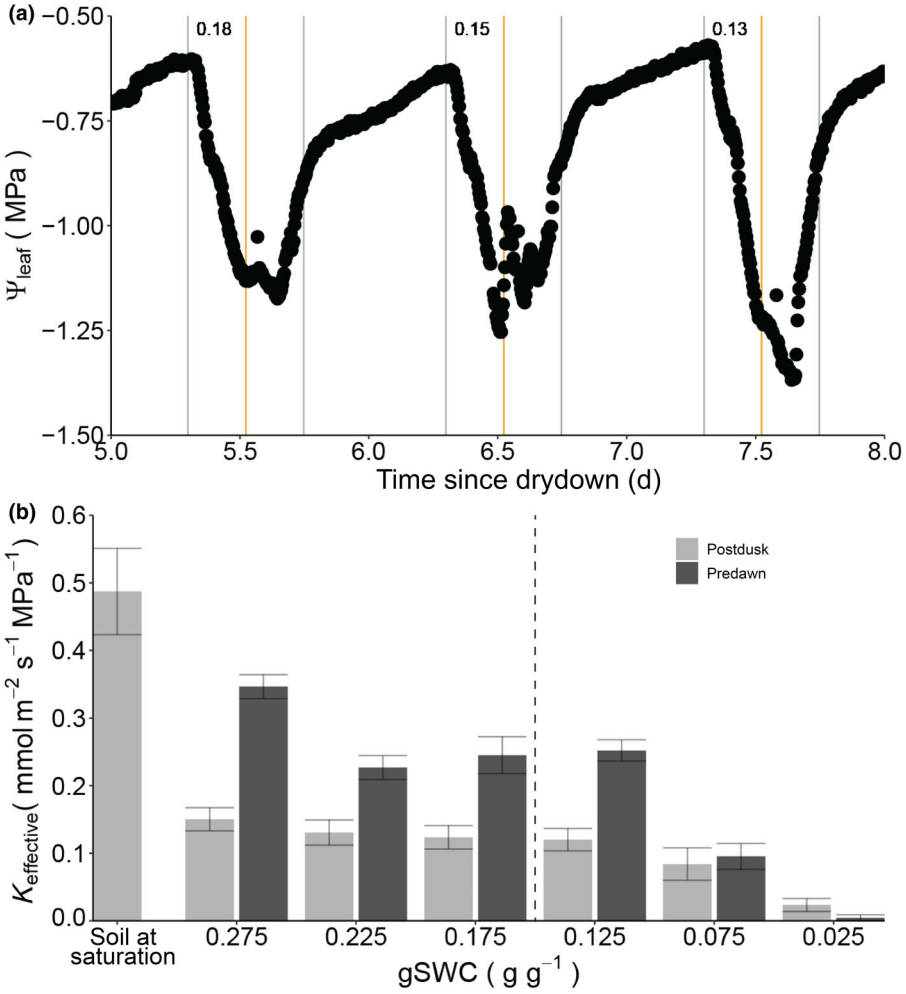


Fig. 3 (a) Representative trace of continuous dendrometer-measured leaf water potential (Ψ_{leaf}) for one plant of *Callitris tuberculata* over a 3-d period, during which the gravimetric soil water content (gSWC) decreased past the threshold of transpiration decline at 0.14 g g^{-1} gSWC. Day and night periods are delineated by vertical lines at dawn and dusk, solar midday is noted each day by vertical yellow lines. The gSWC of the pot is given at the top-right side of the gray dawn line for each day. (b) The plant effect hydraulic conductance ($K_{effective}$) upstream of the dendrometer, for *C. tuberculata* plants in saturated soil ($n = 5$, ±SE) after stomatal closure (postdusk) and during drought at two timepoints per night, postdusk and predawn, binned by gSWC ($n = 5$, ±SE). The dashed line indicates the range of gSWC at which transpiration begins to decline.

Soil-to-plant hydraulic resistance increases late in drought

The resistance to water flow from the plant to the soil remained low over the range of gSWC where transpiration declines, and stomata become fully closed (Fig. 4). The resistance to water flow from the plant into soil only increased once the soil dried beyond 0.05 gSWC (Fig. 4). This flow of water was moving through the root–soil interface, since the uptake rate of water through the plant was significantly higher when the roots were surrounded by soil, compared with when the root systems were soil-free (Fig. S7). For plants with soil, the uptake rate initially increased as Ψ_{pd} decreased from −0.57 to −2.0 MPa. The plant–soil uptake rate stabilized among plants sampled at Ψ_{pd} values more negative than −2.0 MPa. The uptake rate into soil-free roots was consistently low.

Canopy conductance declines occurred at a much higher gSWC than when embolism formed in the stems of glasshouse-grown individuals of *C. tuberculata*. We found that 50% of stem xylem embolism occurred at a mean Ψ_{leaf} of -7.5 ± 1.4 MPa (Fig. 5 inset). In terms of gSWC, 50% of xylem was embolized at the mean value of 0.016 g $g^{-1} \pm 0.016$ (SE) gSWC (Fig. 5). The first 10% of stem xylem was embolized at a gSWC 0.05 g g^{-1}.

Discussion

We find that a recoverable, daily decline in soil hydraulic conductance in close proximity to the roots is the most likely driver of a decline in transpiration during drought (Fig. 6). Modelling suggests that during drought, a stress-onset limit (SOL) is reached when this hydraulic conductance reaches a minimum in the SPAC and is the trigger for when stomata begin to close (Abdalla *et al.*, 2022). In support of this, modelling of K_s suggests that declines in K_s occur at relatively high soil water potentials (Fig. S6). As soil water content declines, we observed a strong breakpoint at which transpiration began to decline (Fig. 1). Similar breakpoints have been widely observed across species (Sadras & Milroy, 1996; Sinclair, 2005; Sinclair *et al.*, 2005; Casadebaig *et al.*, 2008). Variation in the soil water content at which this breakpoint occurs is a primary target of plant breeders selecting for increased drought sensitivity within species (Sinclair & Ludlow, 1986; Sinclair, 2005; Shekoofa *et al.*, 2013; Manandhar *et al.*, 2017; Koehler *et al.*, 2023). Our data suggest that once the SOL is reached, turgor pressure in the leaf declines during the day, triggering ABA biosynthesis and initiating the closing of stomata (Figs 1, 2). This increase in midday ABA levels initiates a gradual reduction in g_s. Increased endogenous ABA levels are

© 2024 The Author(s).
New Phytologist © 2024 New Phytologist Foundation.

14698137, 0, Downloaded from https://nph.onlinelibrary.wiley.com/doi/10.1111/nph.20020 by Readcube (Labtiva Inc.), Wiley Online Library on [26/08/2024]. See the Terms and Conditions (https://onlinelibrary.wiley.com/terms-and-conditions) on Wiley Online Library for rules of use; OA articles are governed by the applicable Creative Commons License

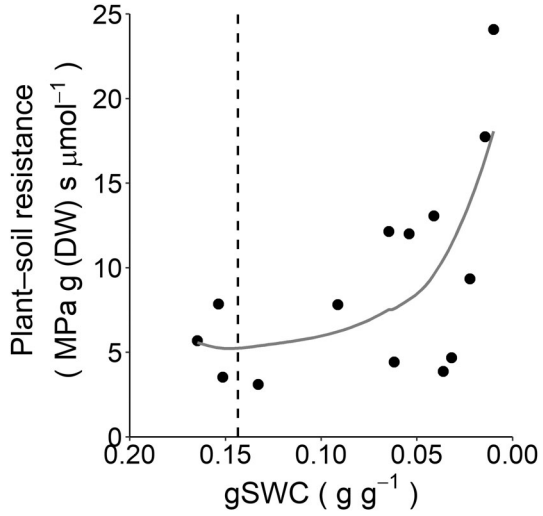


Fig. 4 Plant–soil hydraulic resistance to the uptake of water of *Callitris tuberculata* plants de-topped with roots in soil across varying gravimetric soil water contents (gSWC). The dashed line denotes the gSWC at which transpiration began decreasing over a progressive drought. The trend in plant–soil hydraulic resistance ag gSWC declines is represented by a loess (locally linear smoothing) regression.

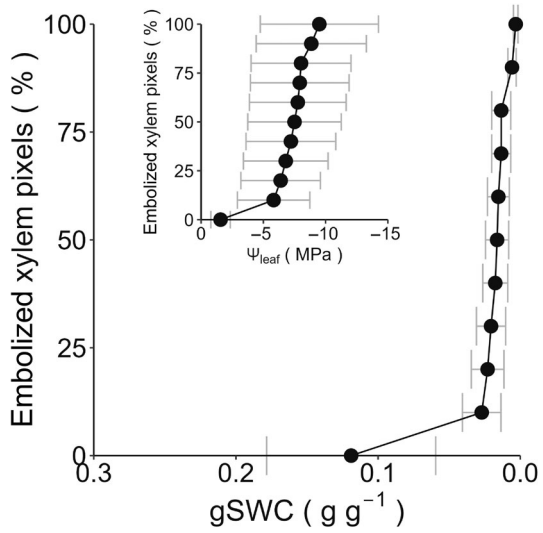


Fig. 5 Optical vulnerability of stem xylem to embolism spread in *Callitris tuberculata*. The closed circles are means ($n = 4$, ±SE) of embolized pixel area plotted against gravimetric soil water content (gSWC). The inset shows that same data plotted against leaf water potential (Ψ_{leaf}).

known to trigger stomatal closure in seed plants, and we show here that increases in foliage ABA levels in *C. tuberculata* correspond to decreases in transpiration during drought. Similar results have been observed in angiosperms (Manandhar *et al.*, 2023).

Ψ_{pd} has long been used as a key metric to estimate the onset of soil drought stress (Reich & Hinckley, 1989; Prior *et al.*, 1997; Thomas & Eamus, 1999; Koehler *et al.*, 2022). Yet here we found that Ψ_{pd} could not be used to accurately predict the timing of when stomata began to close during drought (Fig. 1). This has also been reported in studies that have aimed to predict stomatal closure from differences between Ψ_{md} and Ψ_{pd}, which are only effective at predicting complete stomatal closure (Knipfer *et al.*, 2020). The reason we found Ψ_{pd} could not predict when stomata began to close is that we observed a daily recovery of Ψ_{pd} to maximum values yet saw a gradual decline in transpiration and minimum Ψ_{md} as drought progressed (Fig. 2). This increasing differential between Ψ_{md} and Ψ_{pd} during drought has been observed before (Knipfer *et al.*, 2020). We hypothesize that this increasing decline in Ψ_{md} provides a sufficient decline in daily Ψ_p to trigger ABA biosynthesis which closes stomata. ABA biosynthesis is triggered by a decline in mesophyll cell turgor pressure (Pierce & Raschke, 1980, 1981; McAdam & Brodribb, 2016). And since in *C. tuberculata*, ABA synthesis occurs long before turgor loss point is reached (Figs 1, 2, S2), Ψ_{leaf} at turgor loss point is also not sufficient to predict when stomata begin to close. ABA biosynthesis began with increasing gradients in Ψ_{leaf} that recovered by predawn. There are several potential explanations for why we observed an increasing daily decline, yet nighttime recovery of plant water status in the early stages of drought.

This decline in Ψ_{md} was not due to embolism formation and recovery, because embolism refilling under tension has not been observed in conifers (Choat *et al.*, 2015; Rehschuh *et al.*, 2020), and the mean water potential at which 50% of the stem xylem was embolized (P_{50}) in our plants was −7.5 MPa (Fig. 5). This is a higher P_{50} for this species than what has been measured using the centrifuge from field collected branches, where P_{50} was found to be −18.8 MPa (Larter *et al.*, 2017). Intraspecific variation in embolism resistance has been attributed to growing conditions, with more vulnerable xylem developing under well-watered mesic conditions (Cardoso *et al.*, 2018; Sorek *et al.*, 2022). In some deciduous trees, P_{50} has been observed to decline up to threefold over the season in response to drier conditions (Sorek *et al.*, 2022), and this is within the range of P_{50} values between our recently reproductively mature, glasshouse-grown, individuals of *C. tuberculata* and the field grown mature trees of this species measured by Larter *et al.* (2017). Even with the comparatively vulnerable xylem found in *C. tuberculata*, grown in our experimental conditions, hydraulic failure of the xylem cannot be the cause of daily declines in Ψ_{leaf} during drought. Furthermore, in species with highly vulnerable xylem, like herbaceous crops, we would still expect stomatal closure to occur before embolism formation (Brodribb & McAdam, 2017), but for there to be a narrower gradient in both Ψ_{leaf} and time to occur between the onset of stomatal closure and leaf death.

The recovery of daily plant water status cannot be attributed to any anatomical changes to the root, such as lacunae formation in the cortex, because these do not recover diurnally (Cuneo *et al.*, 2016), requiring new root growth to recover function. Another possibility is that roots are losing connection to the soil (Rodriguez-Dominguez & Brodribb, 2020; Bourbia *et al.*, 2021), yet this loss of K_i is seen to only recover upon re-watering. Studies with observations of recoverable belowground conductance upon re-watering hypothesize that K_{root} is a function of reversible shrinkage of cortical cells, and/or increased hydrophobicity, where K_{root} recovery depends on species, with herbaceous species having immediate recovery compared with woody K_{root}

© 2024 The Author(s).
New Phytologist © 2024 New Phytologist Foundation.

14698137, 0, Downloaded from https://nph.onlinelibrary.wiley.com/doi/10.1111/nph.20020 by Readcube (Labtiva Inc.), Wiley Online Library on [26/08/2024]. See the Terms and Conditions (https://onlinelibrary.wiley.com/terms-and-conditions) on Wiley Online Library for rules of use; OA articles are governed by the applicable Creative Commons License

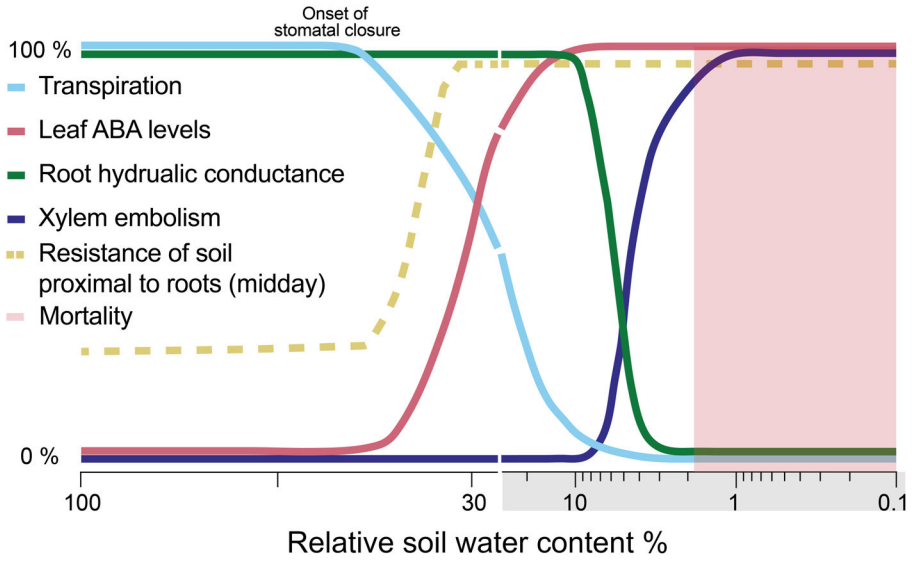


Fig. 6 Schematic representation of the sequence of functional response to decreasing soil water content in seed plants. As soil water content decreases, transpiration remains at maximum until increases in midday soil hydraulic resistance in the closest proximity to the roots triggers downstream decreases in leaf water potentials and leaf endogenous abscisic acid (ABA) biosynthesis, which closes stomata and reduces transpiration. Soil hydraulic resistance in close proximity to the roots reaches a daily maximum triggering stomatal closure via ABA but recovers overnight. Once triggered, transpiration decreases linearly with soil water content as ABA levels increase. When transpiration levels reach a minimum, soil hydraulic resistance is no longer dynamic and reversible overnight, and most of the transpirable soil water has been extracted from the soil; this portion of the figure is expressed in log scale. Without a return to hydrated conditions from this point xylem embolism propagates, root hydraulic conductance declines and plants die.

recovery spanning a number of days (Bourbia *et al.*, 2021). We found that the roots of *C. tuberculata* maintain a near continuous hydraulic connection to the soil as gSWC declined, and that this connection is only lost when plant water status declines to levels when embolism beings to form in the xylem (Fig. 4). Meaning in our study, K_i remained constant for most of the drought and only decreased after embolism formation and permanent declines in $K_{effective}$.

The other potential site of daily resistance to water flow from soil to leaf and hence a variable $K_{effective}$ is a decrease in K_s at relatively high water potentials (Carminati *et al.*, 2020). A heterogenous distribution of water in the soil during drought has been hypothesized (Gardner, 1960; Carminati *et al.*, 2020), but the daily dynamics of water status in the soil closest to the roots remains theoretical (Zarebanadkouki *et al.*, 2016). Our continuous Ψ_{leaf} data show slow nightly recovery of Ψ_{leaf} when gSWC declines, but not in plants in which gSWC is high, in which recovery is rapid (Figs 3, S3). This suggests a nightly recovery of resistance to flow between the water supply in the soil and the leaf. This resistance cannot occur within the plant itself since the slow recovery of Ψ_{leaf} does not occur in saturated soils (Fig. S3). There are studies that propose that drought-induced changes in aquaporin regulation can tune diurnal root hydraulic conductance (Vandeleur *et al.*, 2009; Li *et al.*, 2014). Though with the range of variable aquaporins, it remains difficult to associate particular aquaporin regulation specifically to overnight recovery of belowground hydraulic conductance. In most studies, root aquaporin levels remain constant overnight and only increase with light (Beaudette *et al.*, 2007; Sakurai-Ishikawa *et al.*, 2011) and we found that the application of silver nitrate, a known aquaporin inhibitor (Niemietz & Tyerman, 2002), to hydroponically maintained *C. tuberculata* did not change the nighttime relaxation of Ψ_{leaf} (Fig. S8). Our results suggest that root aquaporin expression or function cannot explain nightly increases in $K_{effective}$.

A dynamic outside plant resistance is the most likely limiter to the conductance through the SPAC as gSWC declines, whereby Ψ_{leaf} is determined by a daily cycle of $K_{effective}$ driven by daily cycles of effective K_s, which declines through the day and recovers before dawn (Fig. 3). It is most likely that this daily cycle of effective K_s is driven by hydraulic recharge of the soil in closest proximity to the roots that had been depleted by daytime transpiration. Consequently, our results support the concept that plants grown under different soil textures, with different soil hydraulic properties, should display variation in the key thresholds of whole plant conductance that regulate hormone levels and stomatal response to declining SWC (Cai *et al.*, 2022; Koehler *et al.*, 2024).

Conclusion

We suggest that the key resistance in the SPAC that primarily drives early declines in midday Ψ_{leaf}, triggering ABA biosynthesis, and therefore, the onset of stomatal closure during drought is in the soil closest to the roots. We found that *C. tuberculata* plants maintain a strong hydraulic connection to the soil, which only collapses once embolism forms under extremely low gSWC. Our study suggests that there is limited, if any, dynamic hydraulic resistor within the plant through drought in this species; this allows stomata to be directly sensitive to changes in soil water

© 2024 The Author(s).
New Phytologist © 2024 New Phytologist Foundation.

14698137, 0, Downloaded from https://nph.onlinelibrary.wiley.com/doi/10.1111/nph.20020 by Readcube (Labtiva Inc.), Wiley Online Library on [26/08/2024]. See the Terms and Conditions (https://onlinelibrary.wiley.com/terms-and-conditions) on Wiley Online Library for rules of use; OA articles are governed by the applicable Creative Commons License

status. Further work is required to understand the hydraulics of this very small region of soil which controls the majority of canopy transpiration dynamics.

Acknowledgements

We thank three reviewers and Tim Brodribb for thoughtful advice, as well as Kean and Cade Kane for helping propagate and maintain plant material. This work was funded by a National Science Foundation grant (IOS-2140119) and USDA National Institute of Food and Agriculture (Hatch project 1014908) to SAMM and Spanish Ministry of Science award (PRE2019-090354) to JP.

Competing interests

None declared.

Author contributions

AM and SAMM designed and performed the research with help from IMR who generated vulnerability curves. TSP and JP helped collect root biomass data. FER contributed to developing the theoretical framework for determining $K_{effective}$ and revised the manuscript, which was written by AM and SAMM. AM conducted the data analysis.

ORCID

Anju Manandhar https://orcid.org/0000-0001-5687-2957
Scott A. M. McAdam https://orcid.org/0000-0002-9625-6750
Javier Pichaco https://orcid.org/0000-0002-5202-9994
Ian M. Rimer https://orcid.org/0000-0002-7727-972X
Fulton E. Rockwell https://orcid.org/0000-0002-2527-6033
Talitha Soares Pereira https://orcid.org/0000-0001-9929-718X

Data availability

All data integral to this study are included in the paper or Supporting Information.

References

Abdalla M, Ahmed MA, Cai G, Wankmüller F, Schwartz N, Litig O, Javaux M, Carminati A. 2022. Stomatal closure during water deficit is controlled by below-ground hydraulics. *Annals of Botany* **129**: 161–170.

Anderegg LDL, Anderegg WRL, Berry JA. 2013. Not all droughts are created equal: translating meteorological drought into woody plant mortality. *Tree Physiology* **33**: 701–712.

Beaudette PC, Chlup M, Yee J, Emery RJN. 2007. Relationships of root conductivity and aquaporin gene expression in *Pisum sativum*: diurnal patterns and the response to $HgCl_2$ and ABA. *Journal of Experimental Botany* **58**: 1291–1300.

Bourbia I, Brodribb TJ. 2024. Stomatal response to VPD is not triggered by changes in soil–leaf hydraulic conductance in Arabidopsis or Callitris. *New Phytologist* **242**: 444–452.

Bourbia I, Pritzkow C, Brodribb TJ. 2021. Herb and conifer roots show similar high sensitivity to water deficit. *Plant Physiology* **186**: 1908–1918.

Brodribb TJ, Carriqui M, Delzon S, Lucani C. 2017. Optical measurement of stem xylem vulnerability. *Plant Physiology* **174**: 2054–2061.

Brodribb TJ, Cochard H. 2009. Hydraulic failure defines the recovery and point of death in water-stressed conifers. *Plant Physiology* **149**: 575–584.

Brodribb TJ, Holbrook NM. 2003. Stomatal closure during leaf dehydration, correlation with other leaf physiological traits. *Plant Physiology* **132**: 2166–2173.

Brodribb TJ, Holbrook NM. 2004. Stomatal protection against hydraulic failure: a comparison of coexisting ferns and angiosperms. *New Phytologist* **162**: 663–670.

Brodribb TJ, Holbrook NM, Edwards EJ, Gutiérrez MV. 2003. Relations between stomatal closure, leaf turgor and xylem vulnerability in eight tropical dry forest trees. *Plant, Cell & Environment* **26**: 443–450.

Brodribb TJ, McAdam SAM. 2017. Evolution of the stomatal regulation of plant water content. *Plant Physiology* **174**: 639–649.

Buckley TN. 2019. How do stomata respond to water status? *New Phytologist* **224**: 21–36.

Cai G, König M, Carminati A, Abdalla M, Javaux M, Wankmüller F, Ahmed MA. 2022. Transpiration response to soil drying and vapor pressure deficit is soil texture specific. *Plant and Soil* **500**: 129–145.

Cardoso AA, Brodribb TJ, Lucani CJ, DaMatta FM, McAdam SAM. 2018. Coordinated plasticity maintains hydraulic safety in sunflower leaves. *Plant, Cell & Environment* **41**: 2567–2576.

Carminati A, Ahmed MA, Zarebanadkouki M, Cai G, Lovric G, Javaux M. 2020. Stomatal closure prevents the drop in soil water potential around roots. *New Phytologist* **226**: 1541–1543.

Carminati A, Javaux M. 2020. Soil rather than xylem vulnerability controls stomatal response to drought. *Trends in Plant Science* **25**: 868–880.

Casadebaig P, Debaeke P, Lecoeur J. 2008. Thresholds for leaf expansion and transpiration response to soil water deficit in a range of sunflower genotypes. *European Journal of Agronomy* **28**: 646–654.

Choat B, Brodersen CR, Mcelrone AJ. 2015. Synchrotron X-ray microtomography of xylem embolism in *Sequoia sempervirens* saplings during cycles of drought and recovery. *New Phytologist* **205**: 1095–1105.

Creek D, Lamarque LJ, Torres-Ruiz JM, Parise C, Burlett R, Tissue DT, Delzon S. 2020. Xylem embolism in leaves does not occur with open stomata: evidence from direct observations using the optical visualization technique. *Journal of Experimental Botany* **71**: 1151–1159.

Cuneo IF, Knipfer T, Brodersen CR, McElrone AJ. 2016. Mechanical failure of fine root cortical cells initiates plant hydraulic decline during drought. *Plant Physiology* **172**: 1669–1678.

Curtis OF. 1926. What is the significance of transpiration? *Science* **63**: 267–271.

Dewar RC. 2002. The Ball-Berry-Leuning and Tardieu-Davies stomatal models: synthesis and extension within a spatially aggregated picture of guard cell function. *Plant, Cell & Environment* **25**: 1383–1398.

Gardner WR. 1960. Dynamic aspects of water availability to plants. *Soil Science* **89**: 63–73.

Harrison Day BL, Johnson KM, Tonet V, Bourbia I, Blackman C, Brodribb TJ. 2023. The root of the problem: diverse vulnerability to xylem cavitation found within the root system of wheat plants. *New Phytologist* **239**: 1239–1252.

Hernandez-Santana V, Rodriguez-Dominguez CM, Fernández JE, Diaz-Espejo A. 2016. Role of leaf hydraulic conductance in the regulation of stomatal conductance in almond and olive in response to water stress. *Tree Physiology* **36**: 725–735.

Hochberg U, Windt CW, Ponomarenko A, Zhang YJ, Gersony J, Rockwell FE, Holbrook NM. 2017. Stomatal closure, basal leaf embolism, and shedding protect the hydraulic integrity of grape stems. *Plant Physiology* **174**: 764–775.

Jain P, Huber AE, Rockwell FE, Sen S, Holbrook NM, Stroock AD. 2023. Localized measurements of water potential reveal large loss of conductance in living tissues of maize leaves. *bioRxiv*. doi: 10.1101/2023.06.06.543905.

Jarvis PG. 1976. The interpretation of the variations in leaf water potential and stomatal conductance found in canopies in the field. *Philosophical Transactions of the Royal Society of London. Series B: Biological Sciences* **273**: 593–610.

Jin Y, Hao G, Hammond WM, Yu K, Liu X, Ye Q, Zhou Z, Wang C. 2023. Aridity-dependent sequence of water potentials for stomatal closure and hydraulic dysfunctions in woody plants. *Global Change Biology* **29**: 2030–2040.

Knipfer T, Bambach N, Isabel Hernandez M, Bartlett MK, Sinclair G, Duong F, Kluepfel DA, McElrone AJ. 2020. Predicting stomatal closure and turgor loss in woody plants using predawn and midday water potential. *Plant Physiology* **184**: 881–894.

© 2024 The Author(s).
New Phytologist © 2024 New Phytologist Foundation.

14698137, 0, Downloaded from https://nph.onlinelibrary.wiley.com/doi/10.1111/nph.20020 by Readcube (Labtiva Inc.), Wiley Online Library on [26/08/2024]. See the Terms and Conditions (https://onlinelibrary.wiley.com/terms-and-conditions) on Wiley Online Library for rules of use; OA articles are governed by the applicable Creative Commons License

Koehler T, Botezatu A, Murugesan T, Kaliamoorthy S, Kholová J, Sadok W, Ahmed MA, Carminati A. 2024. The transpiration rate sensitivity to increasing evaporative demand differs between soil textures, even in wet soil. *Plant Stress* **12**: 100506.

Koehler T, Schaum C, Tung S-Y, Steiner F, Tyborski N, Wild AJ, Akale A, Pausch J, Lueders T, Wolfrum S *et al.* 2022. Above and belowground traits impacting transpiration decline during soil drying in 48 maize (*Zea mays*) genotypes. *Annals of Botany* **131**: 373–386.

Koehler T, Wankmüller FJP, Sadok W, Carminati A. 2023. Transpiration response to soil drying vs. increasing vapor pressure deficit in crops-physical and physiological mechanisms and key plant traits. *Experimental Biology* **74**: 4789–4807.

Larter M, Pfautsch S, Domec JC, Trueba S, Nagalingum N, Delzon S. 2017. Aridity drove the evolution of extreme embolism resistance and the radiation of conifer genus *Callitris*. *New Phytologist* **215**: 97–112.

Li G, Santoni V, Maurel C. 2014. Plant aquaporins: roles in plant physiology. *Biochimica et Biophysica Acta (BBA) – General Subjects* **1840**: 1574–1582.

Manandhar A, Pichaco J, McAdam SAM. 2023. ABA explains the soil water threshold of stomatal regulation during drought. *Authorea*. doi: 10.22541/au.168865599.93826563/v1.

Manandhar A, Sinclair TR, Rufty TW, Ghanem ME. 2017. Leaf expansion and transpiration response to soil drying and recovery among cowpea genotypes. *Crop Science* **57**: 2109–2116.

Martínez-Vilalta J, Garcia-Forner N. 2017. Water potential regulation, stomatal behaviour and hydraulic transport under drought: deconstructing the iso/anisohydric concept. *Plant, Cell & Environment* **40**: 962–976.

Martins SCV, Mcadam SAM, Deans RM, Damatta FM, Brodribb TJ. 2016. Stomatal dynamics are limited by leaf hydraulics in ferns and conifers: results from simultaneous measurements of liquid and vapour fluxes in leaves. *Plant, Cell & Environment* **39**: 694–705.

McAdam SAM, Brodribb TJ. 2016. Linking turgor with ABA biosynthesis: implications for stomatal responses to vapor pressure deficit across land plants. *Plant Physiology* **171**: 2008–2016.

Muggeo VM. 2008. segmented: an R package to fit regression models with broken-line relationships. *R News* **8**: 20–25.

Niemietz CM, Tyerman SD. 2002. New potent inhibitors of aquaporins: silver and gold compounds inhibit aquaporins of plant and human origin. *FEBS Letters* **531**: 443–447.

North GB, Nobel PS. 1991. Changes in hydraulic conductivity and anatomy caused by drying and rewetting roots of *Agave deserti* (Agavaceae). *American Journal of Botany* **78**: 906–915.

Passioura JB. 1988. Water transport in and to roots. *Annual Review of Plant Physiology and Plant Molecular Biology* **39**: 245–265.

Penman HL. 1952. The physical bases of irrigation control. In: *Report of the 13th International Horticultural Congress*. London: Royal Horticultural Society, 913–924.

Pierce M, Raschke K. 1980. Correlation between loss of turgor and accumulation of abscisic acid in detached leaves. *Planta* **148**: 174–182.

Pierce M, Raschke K. 1981. Synthesis and metabolism of abscisic acid in detached leaves of *Phaseolus vulgaris* L. after loss and recovery of turgor. *Planta* **153**: 156–165.

Prior LD, Eamus D, Duff GA. 1997. Seasonal trends in carbon assimilation, stomatal conductance, pre-dawn leaf water potential and growth in *Terminalia ferdinandiana*, a deciduous tree of northern Australian savannas. *Australian Journal of Botany* **45**: 53–69.

Rehschuh R, Cecilia A, Zuber M, Faragó T, Baumbach T, Hartmann H, Jansen S, Mayr S, Ruehr N. 2020. Drought-induced xylem embolism limits the recovery of leaf gas exchange in scots pine. *Plant Physiology* **184**: 852–864.

Reich PB, Hinckley TM. 1989. Influence of pre-dawn water potential and soil-to-leaf hydraulic conductance on maximum daily leaf diffusive conductance in two oak species. *Ecology* **3**: 719–726.

Rockwell FE, Holbrook NM. 2017. Leaf hydraulic architecture and stomatal conductance: a functional perspective. *Plant Physiology* **174**: 1996–2007.

Rodriguez-Dominguez CM, Brodribb TJ. 2020. Declining root water transport drives stomatal closure in olive under moderate water stress. *New Phytologist* **225**: 126–134.

Rodriguez-Dominguez CM, Carins Murphy MR, Lucani C, Brodribb TJ. 2018. Mapping xylem failure in disparate organs of whole plants reveals extreme resistance in olive roots. *New Phytologist* **218**: 1025–1035.

Sadras VO, Milroy SP. 1996. Field crops research soil-water thresholds for the responses of leaf expansion and gas exchange: a review. *Field Crops Research* **47**: 253–266.

Sakurai-Ishikawa J, Murai-Hatano M, Hayashi H, Ahamed A, Fukushi K, Matsumoto T, Kitagawa Y. 2011. Transpiration from shoots triggers diurnal changes in root aquaporin expression. *Plant, Cell & Environment* **34**: 1150–1163.

Scoffoni C, Albuquerque C, Brodersen CR, Townes SV, John GP, Bartlett MK, Buckley TN, McElrone AJ, Sack L. 2017. Outside-xylem vulnerability, not xylem embolism, controls leaf hydraulic decline during dehydration. *Plant Physiology* **173**: 1197–1210.

Scoffoni C, Albuquerque C, Buckley TN, Sack L. 2023. The dynamic multi-functionality of leaf water transport outside the xylem. *New Phytologist* **239**: 2099–2107.

Shatil-Cohen A, Attia Z, Moshelion M. 2011. Bundle-sheath cell regulation of xylem-mesophyll water transport via aquaporins under drought stress: a target of xylem-borne ABA? *The Plant Journal* **67**: 72–80.

Shekoofa A, Mura Devi J, Sinclair TR, Holbrook CC, Isleib TG. 2013. Divergence in drought-resistance traits among parents of recombinant peanut inbred lines. *Crop Science* **53**: 2569–2576.

Sinclair T, Holbrook NM, Zwieniecki M. 2005. Daily transpiration rates of woody species on drying soil. *Tree Physiology* **24**: 1469–1472.

Sinclair TR. 2005. Theoretical analysis of soil and plant traits influencing daily plant water flux on drying soils. *Agronomy Journal* **97**: 1148–1152.

Sinclair TR, Ludlow MM. 1986. Influence of soil water supply on the plant water balance of four tropical grain legumes. *Australian Journal of Plant Physiology* **13**: 329–341.

Skelton RP, Anderegg LDL, Papper P, Reich E, Dawson TE, Kling M, Thompson SE, Diaz J, Ackerly DD. 2019. No local adaptation in leaf or stem xylem vulnerability to embolism, but consistent vulnerability segmentation in a North American oak. *New Phytologist* **223**: 1296–1306.

Smith-Martin CM, Skelton RP, Johnson KM, Lucani C, Brodribb TJ. 2020. Lack of vulnerability segmentation among woody species in a diverse dry sclerophyll woodland community. *Functional Ecology* **34**: 777–787.

Sorek Y, Greenstein S, Hochberg U. 2022. Seasonal adjustment of leaf embolism resistance and its importance for hydraulic safety in deciduous trees. *Physiologia Plantarum* **174**: e13785.

Steudle E, Peterson CA. 1998. How does water get through roots? *Journal of Experimental Botany* **49**: 775–788.

Tardieu F, Simonneau T, Parent B. 2015. Modelling the coordination of the controls of stomatal aperture, transpiration, leaf growth, and abscisic acid: update and extension of the Tardieu-Davies model. *Journal of Experimental Botany* **66**: 2227–2237.

Thomas DS, Eamus D. 1999. The influence of predawn leaf water potential on stomatal responses to atmospheric water content at constant Ci and on stem hydraulic conductance and foliar ABA concentrations. *Journal of Experimental Botany* **50**: 243–251.

Torres-Ruiz JM, Diaz-Espejo A, Perez-Martin A, Hernandez-Santana V. 2015. Role of hydraulic and chemical signals in leaves, stems and roots in the stomatal behaviour of olive trees under water stress and recovery conditions. *Tree Physiology* **35**: 415–424.

Trifiló P, Raimondo F, Savi T, Lo Gullo MA, Nardini A. 2016. The contribution of vascular and extra-vascular water pathways to drought-induced decline of leaf hydraulic conductance. *Journal of Experimental Botany* **67**: 5029–5039.

Tyree MT, Hammel HT. 1972. The measurement of the turgor pressure and the water relations of plants by the pressure-bomb technique. *Journal of Experimental Botany* **23**: 267–282.

Vandeleur RK, Mayo G, Shelden MC, Gilliham M, Kaiser BN, Tyerman SD. 2009. The role of plasma membrane intrinsic protein aquaporins in water transport through roots: diurnal and drought stress responses reveal different strategies between isohydric and anisohydric cultivars of grapevine. *Plant Physiology* **149**: 445–460.

Verslues PE, Bailey-Serres J, Brodersen C, Buckley TN, Conti L, Christmann A, Dinneny JR, Grill E, Hayes S, Heckman RW *et al.* 2023. Burning questions

© 2024 The Author(s).
New Phytologist © 2024 New Phytologist Foundation.

14698137, 0, Downloaded from https://nph.onlinelibrary.wiley.com/doi/10.1111/nph.20020 by Readcube (Labtiva Inc.), Wiley Online Library on [26/08/2024]. See the Terms and Conditions (https://onlinelibrary.wiley.com/terms-and-conditions) on Wiley Online Library for rules of use; OA articles are governed by the applicable Creative Commons License

for a warming and changing world: 15 unknowns in plant abiotic stress. *Plant Cell* **35**: 67–108.

Wankmüller FJP, Carminati A. 2022. Stomatal regulation prevents plants from critical water potentials during drought: result of a model linking soil–plant hydraulics to abscisic acid dynamics. *Ecohydrology* **15**: e2386.

Yang Y, Ma X, Yan L, Li Y, Wei S, Teng Z, Zhang H, Tang W, Peng S, Li Y. 2023. Soil–root interface hydraulic conductance determines responses of photosynthesis to drought in rice and wheat. *Plant Physiology* **194**: 376–390.

Zarebanadkouki M, Meunier F, Couvreur V, Cesar J, Javaux M, Carminati A. 2016. Estimation of the hydraulic conductivities of lupine roots by inverse modelling of high-resolution measurements of root water uptake. *Annals of Botany* **118**: 853–864.

Zimmermann HM, Hartmann K, Schreiber L, Steudle E. 2000. Chemical composition of apoplastic transport barriers in relation to radial hydraulic conductivity of corn roots (*Zea mays* L.). *Planta* **210**: 302–311.

Supporting Information

Additional Supporting Information may be found online in the Supporting Information section at the end of the article.

Fig. S1 Relationship between water potential and stem width.

Fig. S2 Pressure–volume curves and water potential and turgor potential relationship.

Fig. S3 Water potential trace in saturated soil.

Fig. S4 Relationship between canopy conductance and gravimetric soil water content.

Fig. S5 Relationship between relative transpiration and foliage ABA levels.

Fig. S6 Modelled soil hydraulic conductivity with declining water potential.

Fig. S7 Uptake rate of water into the stem base in plants with or without soil.

Fig. S8 Water potential traces overnight in hydroponic plants in the presence of $AgNO_3$.

Please note: Wiley is not responsible for the content or functionality of any Supporting Information supplied by the authors. Any queries (other than missing material) should be directed to the *New Phytologist* Central Office.

© 2024 The Author(s).
New Phytologist © 2024 New Phytologist Foundation.

14698137, 0, Downloaded from https://nph.onlinelibrary.wiley.com/doi/10.1111/nph.20020 by Readcube (Labtiva Inc.), Wiley Online Library on [26/08/2024]. See the Terms and Conditions (https://onlinelibrary.wiley.com/terms-and-conditions) on Wiley Online Library for rules of use; OA articles are governed by the applicable Creative Commons License